Self-Organization

DOI: 10.1002/anie.201303565

Panoscopic Structures by Hierarchical Cascade Self-Assembly of Inorganic Surfactants with Magnetic Heads Containing Dysprosium Ions**

Sebastian Polarz, Christian Bährle, Steve Landsmann, and Alexander Klaiber*

The control over structural organization on different length scales is an important prerequisite to interface nanosystems to the macroscale.[1] Depending on the number of structural levels involved and their interconnection, one might describe such materials as hierarchical or even panoscopic (see Figure 1).[2] The formation of mesoscopic, higher-ordered structures requires special tools for positioning and assembling nanosized building blocks.[3] The dimensions of mesoscopic tools are obviously distinct from atomic dimensions or the macroscopic world. One very powerful approach involves the self-organization of materials.[4] While magnetic interactions have already been exploited for the self-organization of nanoparticles, there are only few reports about magnetic forces that guide the formation of supramolecular nanostructures.[5]

Molecular self-organization is very well documented for surfactants, which are broadly used on a multiton scale as detergents, in cosmetics, as emulsification agents, and as phase-transfer catalysts.[6] Furthermore, the development of nanoscience would not have been possible without surfactants because of their capability to stabilize phases with high surface-to-volume ratio.[7] Their special molecular architecture with the two joined parts of very different solvent compatibility is responsible for their concentration-dependent self-organization behavior, including micellization or the formation of mesophases at low concentration, and the formation of lyotropic liquid crystal (LLC) at higher concentration.[8] More than 99% of surfactants applied in a technological context are organic in nature, with head groups such as ammonium (cationic), oligo(ethylene glycol) (neutral), or carboxylic acid (anionic). Therefore, it is highly desirable to equip surfactants with an enhanced set of properties, which is characteristic for transition-metal ions (e.g., different redox states, magnetic momentum, catalytic activity, etc.). In particular, surfactants with magnetic heads appear to be interesting targets, because the additional, magnetic interaction could guide the formation of unique supramolecular structures.

Such inorganic surfactants can be assigned to the larger class of so-called metallomesogens,[9] which can be devided into two classes. Class 1 includes the coordination of a charged

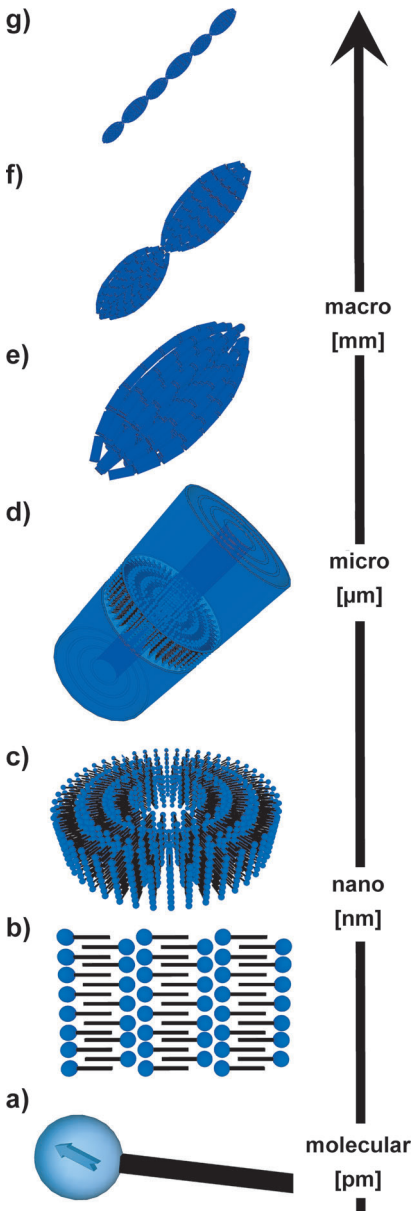

Figure 1. Panoscopic architecture resulting from the hierarchical self-organization of [Dy-C_{10}DOTA] (a). The magnetic moment located at the head group is indicated. b) Lamellar structures with interdigitating inorganic surfactants. c, d) Hollow fibers with multilamellar substructure. e) Tactoid. f) Tactoid dumbbell. g) Chains of tactoids.

[*] Prof. Dr. S. Polarz, C. Bährle, Dr. S. Landsmann, A. Klaiber
Department of Chemistry, University of Konstanz
Universitaetsstrasse 10, 78464 Konstanz (Germany)
E-mail: sebastian.polarz@uni-konstanz.de
Homepage: http://cms.uni-konstanz.de/polarz/

[**] We thank Prof. A. Seubert for assisting us with ICP-AES measurements. Dr. M. Fonin is acknowledged for SQUID measurements.

Supporting information for this article is available on the WWW under http://dx.doi.org/10.1002/anie.201303565.

metal-complex fragment to a chelating organic ligand that bears a hydrophobic chain. In class 2, the metal building block is an integral part of the surfactant.[10]

First examples for class 1 systems were reported by Bruce et al., who developed metal complexes with amines that bear long chains.[11] Le Moigne and Simon were able to combine the metal-binding properties of crown ethers with the design of surfactants.[12] A similar surfactant system and its self-organizing behavior was presented by Neve et al.[13] Bruce and co-workers introduced the pioneering concept of using bipyridine derivatives and related compounds.[14] Zhu and Swager presented a double-tailed surfactant with a vanadyl cation as a magnetic transition-metal center.[15] Binnemans and Görller-Walrand prepared surfactants that contained lanthanides. They presented tailor-made ligands characterized by seven donor centers, which encapsulated the metal ion.[16] Another noteworthy example is the coordination of Gd^{III} with a macrocyclic tetra-aza ligand that was modified with a long alkyl chain, and the application of this compound as a paramagnetic contrast agent in magnetic resonance tomography (MRT).[17]

Here, we report the development of a class 1 system that comprises a head group with a very large magnetic moment. As metal center, we selected Dy^{3+} because of its high magnetic moment, which is the highest among isolated paramagnetic ions (10.48 μ_B). As a ligand, we chose the monoalkylated, decyl-modified 1,4,7,10-tetraazacyclododecane-1,4,7,10-tetraacetic acid (C_{10}DOTA; **1**).[18] We report the synthesis and characterization of a novel inorganic surfactant, and the related panoscopic self-organization process.

Ligand **1** was prepared in accordance with reported methods.[18] It is well soluble in water and behaves as a conventional surfactant (see the Supporting Information, part S-1). Surface tension measurements indicate a critical micelle concentration (*cmc*) of 0.048 mol L^{-1} (23.4 g L^{-1}), which is very high compared to other surfactants, such as SDS (*cmc* = 0.0082 mol L^{-1}). The hydrodynamic diameter of the C_{10}DOTA micelles is $D_H = 3.6$ nm, according to dynamic light scattering (DLS; S-1). At higher temperatures, D_H drops to 2.6 nm, indicating dissolution of the micelles, a process that is reversible. Ligand **1** forms LLC phases at higher concentrations, which can be confirmed by polarization microscopy and small-angle X-ray scattering (SAXS). The data are consistent with a lamellar structure with a periodicity $a =$ 3.48 nm.

Next, C_{10}DOTA was reacted with $Dy^{III}Cl_3$ in methanol by heating to reflux for 48 hours. The characterization of the resulting coordination compound [Dy-C_{10}DOTA] (**2**; Figure 2c) was very difficult, because the paramagnetic character prohibited the application of NMR spectroscopy and the long, flexible alkyl chain impeded the growth of single crystals for X-ray diffraction analysis. EPR spectroscopy failed because of the rapid relaxation times of Dy^{3+}, even at very low temperatures, such as 4 K.[19] However, the successful coordination was confirmed by electron spray ionization mass spectrometry (ESI-MS). A signal at 244 *m*/*z* in the ESI-MS spectrum of the ligand (Figure 2a) could be assigned to a doubly protonated species $[C_{10}DOTA{\cdot}2H]^{2+}$. The distance

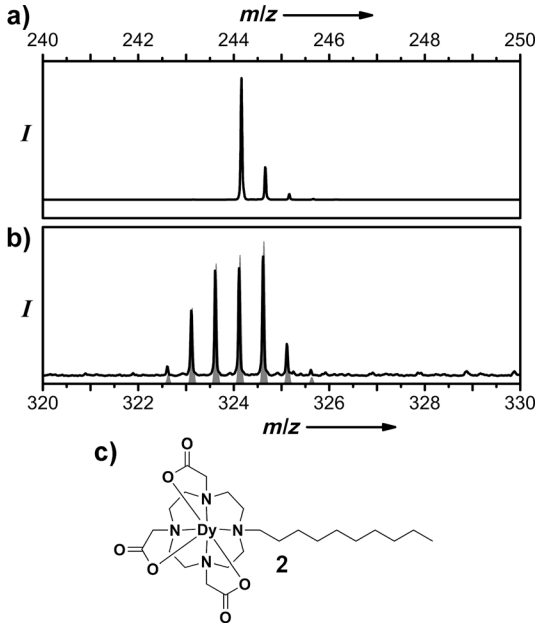

Figure 2. ESI-MS data of the C_{10}DOTA system prior (a) and after (b) reaction with $DyCl_3$ (black graphs: experimental data, grey graph: simulated data). c) Structure of the resulting Dy^{3+}-containing inorganic surfactant.

between the isotope signals of only 0.5 *m*/*z* confirmed the value $z = 2$. After treatment with $DyCl_3$, an analogous new signal for $[Dy\text{-}C_{10}DOTA{\cdot}2H]^{2+}$ could be identified at $m/z =$ 324.6 (Figure 2b). Simulation of the expected ESI-MS pattern gave final evidence that the desired compound was formed. Furthermore, the shift of the C=O vibration from 1677 cm^{-1} to 1584 cm^{-1} for the free acid of C_{10}DOTA (IR spectroscopy) was also indicative of the successful coordination of the ligand to Dy^{3+} (Supporting Information, part S-2). In addition, the related molecular formula of the compound ($C_{24}H_{43}N_4O_6Dy$) was confirmed by a variety of methods, such as elemental analysis, energy dispersive X-ray spectroscopy (EDX), and thermogravimetric analysis (TGA; see the Supporting Information).

The behavior of the compound in water is very complex and was thus studied in detail. The solubility of [Dy-C_{10}DOTA] is quite low ($c_{sol} = 0.5$ mg mL^{-1}) and depends on the pH value. DLS results indicated that the temperature is also highly important. Only very small aggregates exist between $T = 20$–60 °C (see Figure 3a). As the hydrodynamic diameter of these aggregates ($D_h \approx 4$ nm) is about double the length of [Dy-C_{10}DOTA] units, it is very likely that micelles were formed. Micellization could also be confirmed by transmission electron microscopy (TEM; Supporting Information, part S-3), which showed dark spherical objects with an average diameter of 4 nm. Increasing the temperature to 80 °C induced a growth process, and structures with a size of around 210 nm were formed quickly according to DLS analysis (Figure 3a). When the solution was cooled to room temperature, a dispersion of macrosized objects was formed within 2 days. Closer inspection of these objects using light microscopy showed a surprising result. The dispersion was full of dumbbell-shaped aggregates with frayed, moustache-like

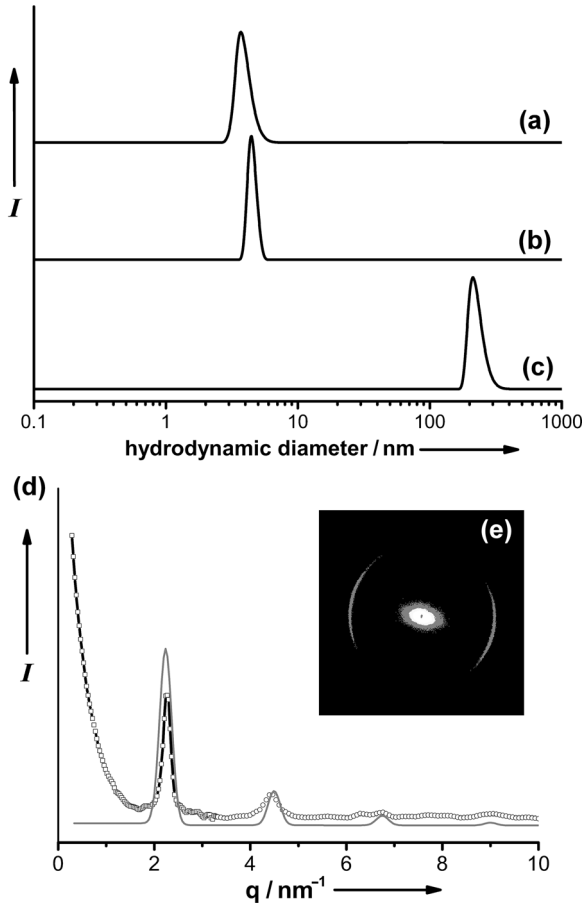

Figure 3. DLS data of [Dy-C_{10}DOTA] in water at $T = 20\,°C$ (a), 60 °C (b), and 80 °C (c). d) Combined SAXS (squares) and WAXS data (circles), together with simulation of scattering data (grey line). e) Two-dimensional SAXS pattern.

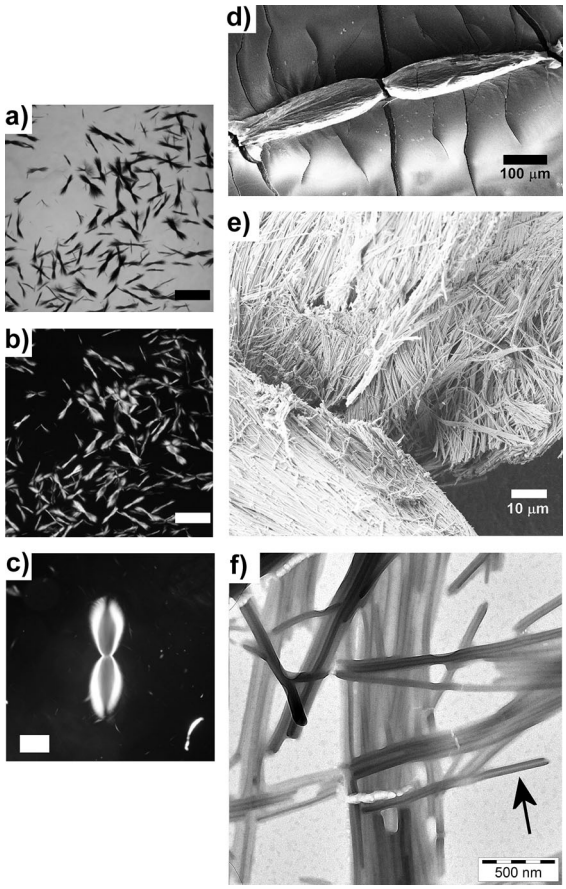

Figure 4. Optical (a) and polarization microscopy (b,c) of the dumbbell aggregates formed by [Dy-C_{10}DOTA]. Scale bar (a,b): 0.5 mm; scale bar (c): 100 μm (see also S-4). d,e) SEM micrographs taken at two different magnifications. f) TEM data (the black arrow marks an isolated fiber).

ends (Figure 4a). The aggregates appeared very bright using crossed polarizers (Figure 4b). The latter result can only be explained by an optical and structural anisotropy. In particular, the inhomogeneous distribution of birefringence in a single dumbbell (Figure 4c) indicated that there might be a more refined architecture on a smaller length scale. Consequently, we studied the materials with additional techniques, such as electron microscopy and SAXS.

Scanning electron microscopy (SEM) data are shown in Figure 4d,e. The particles contain Dy, which was confirmed by EDX (Supporting Information, part S-4). Furthermore, the measurements offer valuable information about the [Dy-C_{10}DOTA] aggregates. For example, the dumbbells consist of numerous fibers, of which most are aligned parallel to each other and parallel to the long axis of the particle. The length of the fibers is in the range of several micrometers. Next, TEM was performed (Figure 4f), showing that a single fiber has a diameter of around 56 nm, and also the presence of bundles containing several fibers. Each fiber seems to have a hollow substructure with approximately 18 nm thick 'walls'. The large thickness makes it difficult to identify smaller structures using TEM. However, lamellar characteristics can be identified in the respective micrographs (S-4). Furthermore, fast Fourier transform (FFT) analysis indicated a lamellar structure with a periodicity of $a = 2.9$ nm. SAXS measurements confirmed the results, and the data were complemented by an additional experiment to address the wide-angle region (WAXS; data shown in Figure 3b). The pattern can also be explained by a lamellar structure with a layer-to-layer distance of $a = 2.8$ nm. Because this distance is less than double the length of one [Dy-C_{10}DOTA] unit, it can be assumed that partial interdigitation has taken place. Interdigitation of the alkyl chains in surfactant aggregates is a known phenomenon, originating from subtle differences in head-group interaction.[20] It should also be noted that the 2-D SAXS pattern (Figure 3c) is asymmetric, which is a clear sign for a preferential orientation of the layers in the lamellar substructure.

A direct comparison of [Dy-C_{10}DOTA] with C_{10}DOTA confirmed that the presence of Dy^{3+} is responsible for the unique cascade of self-organization steps (Figure 1). As C_{10}DOTA, [Dy-C_{10}DOTA] assembled into lamellar structures first. However, a small but important difference is the smaller interlamellar distance ($\Delta a = -0.68$ nm) in [Dy-C_{10}DOTA]. This evidence suggests an enhanced, presumably magnetic interaction between the heads of **2**. It is also well known that lamellar surfactant systems have a tendency to form multi-

walled vesicles.[21] [Dy-C_{10}DOTA] is different, because it does not form ordinary, spherical vesicles, but instead forms hollow fibers (Figure 1 c,d). Again, the latter finding and also the length of these fibers is indicative of an additional, strong and anisotropic (!) interaction. The anisotropy at the nanoscale level was clearly shown by SAXS (Figure 3 c). The fact that the fibers assemble further into elliptical particles confirmed the existence of a factor responsible for a long-range ordering. Similar phenomena have only been reported rarely. Kniep et al. described the formation of hierarchical fluoroapatite particles in gelatine gel.[22] They also found that fractal growth was influenced by a number of factors, including long-range electrostatic interactions.[23] Another spectacular example was the emergence of V_2O_5 tactoids.[24] The V_2O_5 system is similar to [Dy-C_{10}DOTA] in some respects. V_2O_5 possesses a lamellar crystal structure, elongated particles form easily, and the particles form bundles, which organize into elliptical particles. The differences are that V^{IV} is diamagnetic and the dumbbell morphology (Figure 1 f) could not be observed for V_2O_5 mesoscopic materials.

The previous assumption that a magnetic interaction plays a crucial role during the presented self-organization processes is supported as follows. First, analogous experiments were performed with the diamagnetic Lu^{3+} (instead of Dy^{3+}) and C_{10}DOTA. We could at no time observe the formation of any large-structure precipitates, neither at room temperature, nor after heating to 80 °C followed by cooling. Only dispersions of micelles were found (data not shown). Second, when a static magnetic field was present during the formation of the tactoids, microscopy data show the introduction of an additional level of structural complexity (Figures 5 c and 1 g). Many of the single tactoids have aligned into chain-like structures.

Obviously, it was necessary to investigate the magnetic properties of the material, and superconducting quantum interference device (SQUID) measurements were thus performed (Figure 6). Measurements of the magnetization at room temperature showed a linear dependency on the applied magnetic field (Figure 6 b). The magnetization M is not saturated at high fields, also because of relaxation features of Dy^{3+}.[19] The sign of the magnetic susceptibility χ is positive, given as the slope of the magnetization curve. The system is paramagnetic. Because the exact volume and density of the complex self-assembled [Dy-C_{10}DOTA] structures could not be given, determination of the value for the molar magnetic susceptibility χ_m was unfortunately not possible at this point. However, the latter conclusion regarding the paramagnetic nature was supported by temperature-dependent measurements (Figure 6 a). In particular the $1/M$ versus T plot confirmed that the current data set obeys the Curie–Weiss law perfectly. Considering the magnetic measurement, one might think that the magnetic features of the materials are trivial. However, the opposite is the case. The field of a weak external magnet (< 1 T $\approx$ equal to a commercially available permanent magnet) was sufficient for instantaneous manipulation of the tactoid structures (see Figure 5 and the Supporting Information, S-5). All structures aligned with the magnetic field as soon as it was applied. In this sense, the materials behaved similar to superparamagnetic species, such as Fe_3O_4 (magnetite) nanoparticles. Superparamagnetic colloids are also known as ferrofluids.[25] Although their magnetic behavior is paramagnetic, it is possible to control their movement using small magnetic fields.

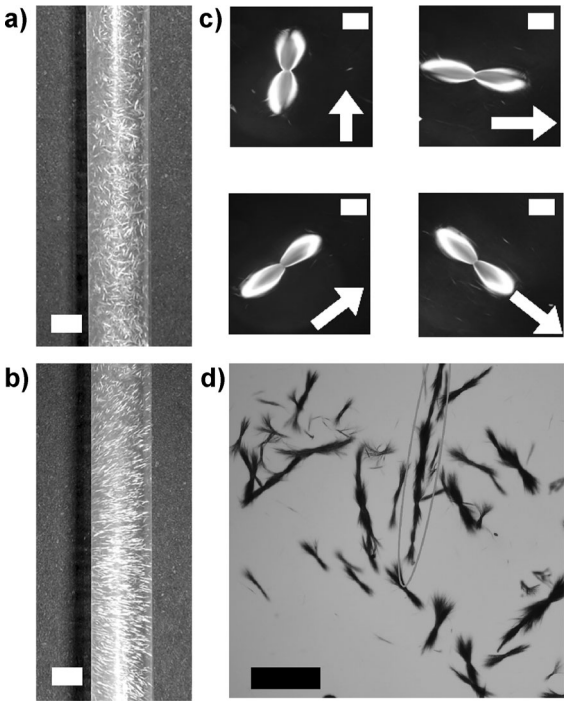

Figure 5. a) Photographic images of randomly oriented [Dy-C_{10}DOTA] tactoids in the absence of a magnetic field. b) Orientation takes places when a field is applied. Scale bar: 2.5 mm. c) Polarization microscopy images of one particle and its alignment in the direction of the magnetic field (indicated by the white arrow) present during the measurement. Scale bar: 100 μm. d) Chain-like tactoid structures, obtained by growth in the presence of a static magnetic field. Scale bar: 0.5 mm.

It can be concluded that the properties of the self-organized [Dy-C_{10}DOTA] structures go beyond simple paramagnetism. In order to understand this phenomenon, it was necessary to consider magnetic anisotropy caused by splitting of the Dy metal orbitals because of ligand-field effects. In general, a molecule will align to an externally applied magnetic field B_0 if its magnetic susceptibility is anisotropic, that is, $\chi_\perp \neq \chi_\parallel$ ($\parallel$: parallel alignment to B_0; $\perp$: orthogonal alignment).[26] Furthermore, the mentioned effect can amplify, if such molecular objects are aligned into a defined structure, which is also anisotropic. In the current case, it was the formation of the lamellar LLC phase that initiated the structure formation process. Next, nanorod building blocks with a significant structural magnetic anisotropy were formed. While the latter explanations rationalize, why it is possible to manipulate the system by applying an external magnetic field, it is an open question, what exactly triggers the formation of the tactoids, and which factor is responsible for the pairing of the tactoids into dumbbells. Therefore, elucidating the formation mechanism will be subject to future research.

In summary, the self-organization of the inorganic surfactant [Dy-C_{10}DOTA] is very complex and hierarchical (see Figure 1). The current work represents one of the first

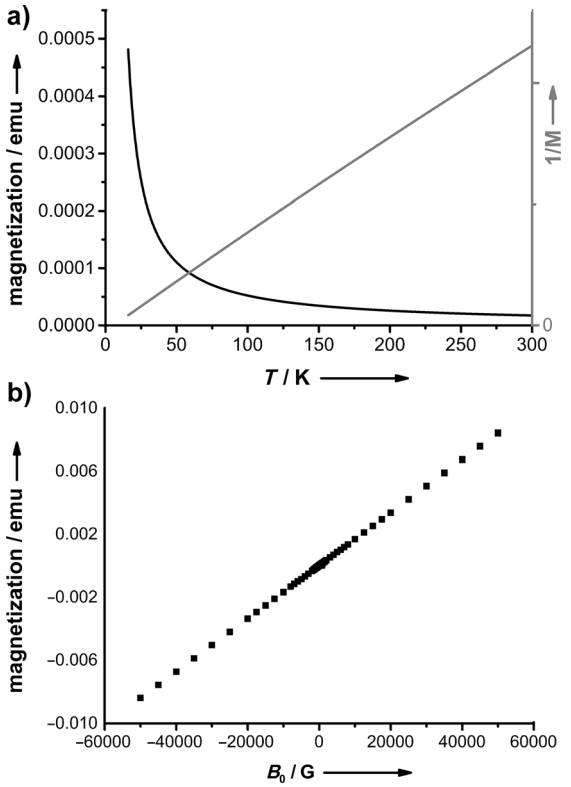

Figure 6. Magnetization curves determined by SQUID measurements. a) Temperature-dependency; linear plot (black graph) and Curie–Weiss plot (grey graph). b) Field-dependent magnetization at room temperature.

examples for amphiphilic structures with panoscopic features and for self-organization processes of surfactants driven by long-range magnetic interactions. The head group of this inorganic surfactant contains a large magnetic momentum, which is the main difference to conventional systems. As a result, it is possible to control the nano-[Dy-C_{10}DOTA] system by an external, macroscopic trigger, which should be interesting for potential applications.

Experimental Section

C_{10}DOTA was prepared according to published procedures.[18b] Complexation of Dy^{3+} was achieved by reacting C_{10}DOTA (5×10^{-4} mol; 0.243 g) with an equimolar amount of $DyCl_3$(5×10^{-4} mol; 0.134 g) in methanol (10 mL) for 48 h under reflux. Remaining solid residues were filtered off. After the removal of the solvent, the product was obtained as a white solid in quantitative yield.

Details about the analytical methods and procedures are given in the Supporting Information.

Received: April 26, 2013
Revised: July 29, 2013
Published online: October 22, 2013

Keywords: amphiphiles · colloids · liquid crystals · self-organization · supramolecular chemistry

[1] a) O. Ikkala, G. ten Brinke, *Chem. Commun.* **2004**, 2131 – 2137; b) D. B. Kuang, T. Brezesinski, B. Smarsly, *J. Am. Chem. Soc.* **2004**, *126*, 10534 – 10535.
[2] a) J. Aizenberg, J. C. Weaver, M. S. Thanawala, V. C. Sundar, D. E. Morse, P. Fratzl, *Science* **2005**, *309*, 275 – 278; b) P. Fratzl, R. Weinkamer, *Prog. Mater. Sci.* **2007**, *52*, 1263 – 1334.
[3] a) G. A. Ozin, *Chem. Commun.* **2000**, 419 – 432; b) S. Mann, G. A. Ozin, *Nature* **1996**, *382*, 313 – 318.
[4] a) G. Li, V. Shrotriya, J. S. Huang, Y. Yao, T. Moriarty, K. Emery, Y. Yang, *Nat. Mater.* **2005**, *4*, 864 – 868; b) J. M. Lehn, *Science* **2002**, *295*, 2400 – 2403; c) C. B. Murray, C. R. Kagan, M. G. Bawendi, *Science* **1995**, *270*, 1335 – 1338.
[5] a) A. H. Lu, E. L. Salabas, F. Schüth, *Angew. Chem.* **2007**, *119*, 1242 – 1266; *Angew. Chem. Int. Ed.* **2007**, *46*, 1222 – 1244; b) K. J. M. Bishop, C. E. Wilmer, S. Soh, B. A. Grzybowski, *Small* **2009**, *5*, 1600 – 1630.
[6] H. Stache, K. Kosswig, *Surfactant Pocketbook*, 3rd ed., Hanser, Berlin, **1990**.
[7] a) S. Polarz, B. Smarsly, *J. Nanosci. Nanotechnol.* **2002**, *2*, 581 – 612; b) H. Weller, *Curr. Opin. Colloid Interface Sci.* **1998**, *3*, 194 – 199; c) S. Förster, T. Plantenberg, *Angew. Chem.* **2002**, *114*, 712 – 739; *Angew. Chem. Int. Ed.* **2002**, *41*, 688 – 714.
[8] a) R. Nagarajan, E. Ruckenstein, *Langmuir* **1991**, *7*, 2934 – 2969; b) J. N. Israelachvili, *Intermolecular and Surface Forces*, Elsevier, Amsterdam, **2011**.
[9] a) A. M. Giroud-Godquin, P. M. Maitlis, *Angew. Chem.* **1991**, *103*, 370 – 398; *Angew. Chem. Int. Ed. Engl.* **1991**, *30*, 375 – 402; b) S. A. Hudson, P. M. Maitlis, *Chem. Rev.* **1993**, *93*, 861 – 885; c) P. M. Maitlis, D. W. Bruce, R. Dhillon, D. A. Dunmur, F. P. Fanizzi, S. E. Hunt, R. Lelagadec, E. Lalinde, R. Orr, J. P. Rourke, N. J. S. Salt, J. P. Stacey, P. Styring, *New J. Chem.* **1990**, *14*, 549 – 551.
[10] a) S. Landsmann, C. Lizandara-Pueyo, S. Polarz, *J. Am. Chem. Soc.* **2010**, *132*, 5315 – 5321; b) J. J. Giner-Casares, G. Brezesinski, H. Mohwald, S. Landsmann, S. Polarz, *J. Phys. Chem. Lett.* **2012**, *3*, 322 – 326; c) S. Landsmann, M. Luka, S. Polarz, *Nat. Commun.* **2012**, *3*, 1299; d) S. Landsmann, M. Wessig, M. Schmid, H. Cölfen, S. Polarz, *Angew. Chem.* **2012**, *124*, 6097 – 6101; *Angew. Chem. Int. Ed.* **2012**, *51*, 5995 – 5999.
[11] a) D. W. Bruce, D. A. Dunmur, P. M. Maitlis, J. M. Watkins, G. J. T. Tiddy, *Liq. Cryst.* **1992**, *11*, 127 – 133; b) D. W. Bruce, I. R. Denby, G. J. T. Tiddy, J. M. Watkins, *J. Mater. Chem.* **1993**, *3*, 911 – 916.
[12] J. Le Moigne, J. Simon, *J. Phys. Chem.* **1980**, *84*, 170 – 177.
[13] F. Neve, M. Ghedini, G. Demunno, A. M. Levelut, *Chem. Mater.* **1995**, *7*, 688 – 693.
[14] a) D. W. Bruce, J. D. Holbrey, A. R. Tajbakhsh, G. J. T. Tiddy, *J. Mater. Chem.* **1993**, *3*, 905 – 906; b) J. D. Holbrey, G. J. T. Tiddy, D. W. Bruce, *J. Chem. Soc. Dalton Trans.* **1995**, 1769 – 1774.
[15] S. S. Zhu, T. M. Swager, *Adv. Mater.* **1995**, *7*, 280 – 283.
[16] K. Binnemans, C. Görller-Walrand, *Chem. Rev.* **2002**, *102*, 2303 – 2345.
[17] W. C. Baker, M. J. Choi, D. C. Hill, J. L. Thompson, P. A. Petillo, *J. Org. Chem.* **1999**, *64*, 2683 – 2689.
[18] a) J. Massue, S. E. Plush, C. S. Bonnet, D. A. Moore, T. Gunnlaugsson, *Tetrahedron Lett.* **2007**, *48*, 8052 – 8055; b) B. Jagadish, G. L. Brickert-Albrecht, G. S. Nichol, E. A. Mash, N. Raghunand, *Tetrahedron Lett.* **2011**, *52*, 2058 – 2061.
[19] I. Bikchantaev, Y. G. Galyametdinov, O. Kharitonova, I. V. Ovchinnikov, D. W. Bruce, D. A. Dunmur, D. Guillon, B. Heinrich, *Liq. Cryst.* **1996**, *20*, 489 – 492.
[20] M. Kranenburg, M. Venturoli, B. Smit, *J. Phys. Chem. B* **2003**, *107*, 11491 – 11501.
[21] E. W. Kaler, K. L. Herrington, A. K. Murthy, J. A. N. Zasadzinski, *J. Phys. Chem.* **1992**, *96*, 6698 – 6707.

[22] a) R. Kniep, S. Busch, *Angew. Chem.* **1996**, *108*, 2788 – 2791; *Angew. Chem. Int. Ed. Engl.* **1996**, *35*, 2624 – 2626; b) S. Busch, U. Schwarz, R. Kniep, *Adv. Funct. Mater.* **2003**, *13*, 189 – 198.
[23] P. Simon, U. Schwarz, R. Kniep, *J. Mater. Chem.* **2005**, *15*, 4992 – 4996.
[24] a) P. Davidson, C. Bourgaux, L. Schoutteten, P. Sergot, C. Williams, J. Livage, *J. Phys. II* **1995**, *5*, 1577 – 1596; b) A. V. Kaznacheev, M. M. Bogdanov, A. S. Sonin, *J. Exp. Theor. Phys.* **2003**, *97*, 1159 – 1167; c) C. Lausser, H. Cölfen, M. Antonietti, *ACS Nano* **2011**, *5*, 107 – 114.
[25] U. Jeong, X. W. Teng, Y. Wang, H. Yang, Y. N. Xia, *Adv. Mater.* **2007**, *19*, 33 – 60.
[26] Y. G. Galyametdinov, W. Haase, B. Goderis, D. Moors, K. Driesen, R. Van Deun, K. Binnemans, *J. Phys. Chem. B* **2007**, *111*, 13881 – 13885.

